Electron Transfer Kinetics at Single-Layer Graphene/Ionic Liquid Interfaces

Shuai Liu, Guilhem Pignol, Corinne Lagrost, Bingwei Mao, Jiawei Yan, Philippe Hapiot

ChemElectroChem

Research Article
doi.org/10.1002/celc.202300658

Chemistry Europe
European Chemical Societies Publishing

www.chemelectrochem.org

Special Collection

Electron Transfer Kinetics at Single-Layer Graphene/Ionic Liquid Interfaces

Shuai Liu,[a] Guilhem Pignol,[a] Corinne Lagrost,[a] Bingwei Mao,[a] Jiawei Yan,*[a] and Philippe Hapiot*[a]

Electron transfer kinetics at the single-layer graphene/ionic liquids interfaces have been examined for different common imidazolium-based ionic liquids and ferrocene derivatives. The heterogeneous kinetics are characterized by slow standard charge transfer rates and an unusual low variation of the rate with the applied potential corresponding to charge transfer coefficients lower than 0.1. This behavior is specific to the electrochemistry on a single-layer graphene as we found that the oxidation of the same substituted ferrocenes in the same ionic liquids follows the classical behavior predicted by the Butler-Volmer law.

Introduction

Electrochemical properties of graphene/solvent interfaces have attracted a lot of interest in aqueous and organic solvents because of numerous possible applications.[1,2] Graphene is composed by a single atom layer of sp^2 carbon and displays interesting characteristics for electrochemical application because of high electron mobility, zero band gap, nearly transparency and flexibility.[3] These features make graphene a good candidate for use as an electrode materials in electrochemical applications among them, photovoltaics,[4,5] sensing and biosensing application[6] or field-effect transistors.[7] Some basic studies of the electrochemical properties of graphene concern the heterogeneous charge transfer kinetics between graphene and molecules in solution that is a key parameter for most applications in electrochemistry.[1,2,8,9,10,11,12] In the field of attractive solvents for electrochemistry, Room Temperature Ionic Liquids (RTILs) have been deserving a special attention in electrochemistry.[13,14] RTILs are a class of solvents consisting primarily of ionic species that have been widely considered in electrochemistry for their advantages, among them are wide electrochemical windows, low vapor pressures and good ionic conductivities. In this context, the graphene/RTIL interface appears as particularly attractive as it could combine the specific properties of RTILs properties with those of graphene leading to a modification of the electrochemical properties thanks to a different interface. For example, using graphene and ionic liquids is commonly considered for numerous applications ranging from catalysis to energy storage applications.[15]

In the present study, we have examined the electron transfer kinetics at graphene/RTIL interfaces for two common imidazolium-based ionic liquids ([EMIM][TFSI] and [BMIM][TFSI]) and a series of ferrocenes derivatives using Scanning Electrochemical Microscopy (SECM). Ferrocene derivatives were chosen because they present high self-exchange charge transfer rate constants and their redox potentials are localized in a region where graphite and graphene possess a significant DOS.[16,17] Both characteristics should lead to high electron transfer rates that are suitable for applications and simplify the studies.[18] Localized electrochemical techniques like SECM or SECCM (Scanning Electrochemical Cell Microscopy) are well adapted to such samples and were efficiently used for investigating the interface of single layer graphene[8–11,19] or basal plan of HOPG[11,12] in aqueous or organic solvents. In those cases, SECM has advantages versus other common electrochemical methods like cyclic voltammetry because samples are generally too large for the technique. SECM provides a view of the heterogeneity of the surface contrarily to cyclic voltammetry that gives only a global view of the sample. Then, we have compared the charge transfer kinetics on a single-layer graphene, on one hand, with the values measured using a classical millimetric gold electrode and the same redox mediators in the same RTILs and, on the other hand, with previously reported kinetics data obtained in aqueous and organic solvents.[9–12]

Experimental Section

Electrochemical Measurements

A Model 920E Scanning Electrochemical Microscope (C.H. Instruments, Austin, TX) was used for all the SECM and for most of the

[a] S. Liu, G. Pignol, C. Lagrost, B. Mao, J. Yan, P. Hapiot
Univ Rennes, CNRS, ISCR - UMR 6226, F-35000 Rennes, France
and
State Key Laboratory of Physical Chemistry of Solid Surfaces and Department of Chemistry, College of Chemistry and Chemical Engineering, Xiamen University, Xiamen 361005, China
E-mail: jwyan@xmu.edu.cn
philippe.hapiot@univ-rennes1.fr

Supporting information for this article is available on the WWW under https://doi.org/10.1002/celc.202300658

Special Collection SC: Flavio Maran Festschrift

electrochemical measurements. A typical three-electrode or four-electrode setup was used in all electrochemical measurements, with a platinum counter electrode and a quasi-reference electrode. The SECM setup is equipped with an adjustable stage for the tilt angle correction and placed on a vibration isolation platform. The applied potential at the microelectrode tip is chosen as being sufficiently positive (or negative) to ensure a fast electron transfer at the tip. The tip electrode was made following the method proposed by Bard using the micropipette laser puller P2000 (Sutter Instrument, Novato CA).[20] Experimental data were analyzed with the approximation proposed by Lefrou *et al*,[21] all the experiments were performed using the same SECM probe, with a geometry determined as r = 3.7 um with RG = 12.7 using the irreversible oxidation of anthracene prior measurement.[22]

Electrical contact to the graphene substrate was made with copper tape containing conductive adhesive (Saint-Gobain Performance Plastics). The typical resistance in the contact between the copper and graphene was measured around 5–10 kΩ, which was mostly due to the resistance across the graphene layer, as measured across *ca.* 1 cm of the graphene. Electrodes were placed inside a Teflon cell, and an O-ring was used to expose an area of around 0.5 cm^2 of the graphene layer to the RTIL solution. Tilt angle on large SECM images was corrected with Gwyddion software.[23]

For measurements on a 1-mm diameter disk gold electrode, the standard heterogeneous electron transfer rate constants, k_s in the RTILs were measured by fast-cyclic voltammetry through comparison of the experimental data with calculated curves assuming a Butler-Volmer law and an α transfer coefficient $\alpha = 0.5$ following a previously published procedure.[23] The working electrode was a 1 mm-diameter disk gold electrode and a 0.5 mm-diameter platinum wire was used as a quasi-reference electrode. All the fast-cyclic voltammetry experiments were performed using a homemade potentiostat equipped with an electronic positive feedback compensation of the ohmic drop.[24] As discussed previously, an efficient compensation of the ohmic drop for cyclic voltammetry experiments in RTILs is a requirement for performing such measurements and avoid a strong underestimation of k_s. The diffusion coefficients of the redox probes were measured by cyclic voltammetry according to classical method considering a reversible electron transfer.[25] All the experiments were performed at 45 °C with a homemade heating system.

Chemicals and materials

The RTILs, 1-ethyl-3-methylimidazolium bis(trifluoromethylsulfonyl)imide [EMIM][TFSI] and 1-butyl-3-methylimidazolium bis (trifluoromethylsulfonyl)imide [BMIM][TFSI], were prepared from aqueous $LiN(CF_3SO_2)_2$, LiTFSI (Solvionic), and the imidazolium-based chloride salts (Thermo Scientifics) salts according to standard procedures.[26] The samples were purified by extensive washing in ultrapure water (18.2 MΩ, Prelab Flex, Veolia) and filtered over neutral alumina and silica. The three mediators: ferrocene (Fc), ferrocene-methanol (FcMeOH), and ferrocene-dimethanol $Fc(MeOH)_2$ (Sigma-Aldrich) were used as received unless noted otherwise. Single-layer graphene was purchased from Nanjing JI Cang Nano Technology Co. Ltd., whose quality was examined by atomic force microscopy (AFM Model 5500, Keysight) and Raman spectroscopy (see supporting information).

Results and Discussion

SECM in feedback mode was used to examine the electron transfer kinetics between substituted ferrocenes and a single-layer graphene. In this configuration, the reactive form of the mediator is generated at the tip electrode then diffuses to the graphene layer where it could exchange an electron. SECM has the advantage of providing a local view of the electrochemical reactivities and is especially useful for sample where making an electrode could be complicated.[8,9] First, SECM images of the graphene in the RTILs were recorded in unbiased conditions. The tip-substate distance is maintained constant and the graphene is not connected. In all SECM experiments, the potentials applied at the tip were chosen to be at least 300 mV more positive than the mediator standard potential, $E°$, to ensure that there is no kinetic limitation due to electron transfers at the tip. This simplest configuration allows testing of the graphene homogeneity and selecting a convenient position to record the approach curves after identification of an area with no defect. At this point, we must also highlight that making experiments in ionic liquids requires some additional care because of the higher viscosity of the media. The diffusion coefficients are thus lower than in classical electrolyte and thus it takes more time for the system to reach a "radial diffusion" steady state. This was illustrated in previous publications,[27,28] experimentally, this could appear as a change of the approach curve with the approach rate or that the shape of the curve is altered versus the one under real steady state. The real description of the problem is complicated as for a rigorous treatment of SECM, one needs to consider the time for establishing the feedback loop that depends on the feedback character of the approach curve and the possibility that diffusion coefficients are generally not equal for the neutral and oxidized species in ionic liquids.[29] Nevertheless, to check that our experiments were indeed performed under steady state, we performed chronoamperometry and cyclic voltammetry analysis to ensure that the current does not change with time when working at 45 °C. (See Figure S4 in the Supplementary information section).

As seen on Figure 1 with the example of an image recorded using FcMeOH as a mediator in [EMIM][TFSI], large zones of iso-current are observed confirming the quality of the graphene substrate as seen by AFM and Raman spectroscopy (See supporting information part). After choosing the position of the tip over the graphene that corresponds to the highest electrochemical activity, the heterogeneous kinetics were examined by acquiring a series of approach curves at different substrate bias potentials. Practically, we chose first a random position and moved the tip within a range around 200×200 μm to search the most positive feedback curve under the unbiased conditions. Then the approach curves were recorded as a group set at different substrate potentials and the reproducibility of the curves were checked at least 3 times. For the approach curves, i is normalized by the infinite current i_∞ (tip current measured when the tip is localized at an infinite distance). i/i_∞ is then plotted as a function of L with $L = d/a$ where d is the distance between the tip and the graphene

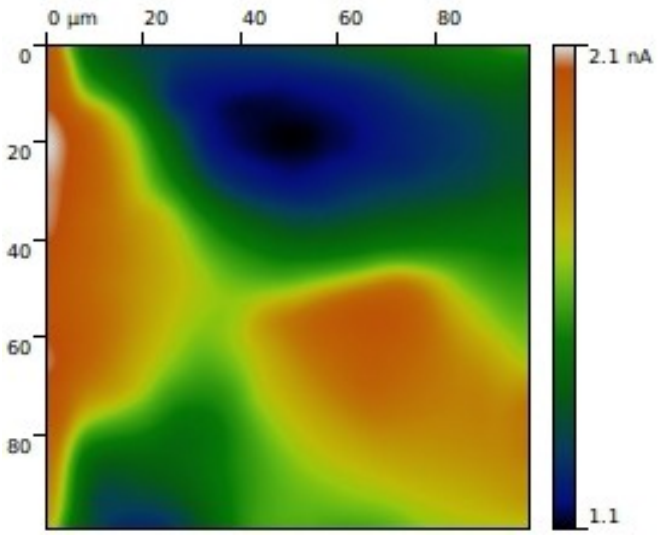

Figure 1. SECM image of single-layer graphene using FcMeOH as a redox probe ($C^{\circ} = 27$ mmol.L^{-1}) in [EMIM][TFSI]. Tip potential was set at the level of the diffusion plateau of the oxidation of FcMeOH and tip to substrate distance was maintained constant around 3 µm to avoid damages on the layer. (Tilt angle was corrected using Gwyddion software).

layer and *a* the radius of the electrode. The position of the Z axis origin of the tip was obtained by recording and fitting an approach curve using the irreversible anthracene oxidation prior to the experiment following a previously described procedure[30] Finally, the approach curves recorded at different potentials were fitted using the finite kinetic model proposed by Lefrou *et al.*[21] providing a measure of the dimensionless parameter $\kappa = k_{el}/aD$ (D is the diffusion coefficient of the mediator and k_{el} is the electron transfer rate constant at the applied potential). Finally, the value of the heterogenous electron transfer k_{el} between the mediator and the graphene layer is derived with the value of D of the ferrocene in the ionic liquid that is measured independently.

As seen on Figure 2 with the examples of FcMeOH in [EMIM][TFSI] and [BMIM][TFSI], a good fitting is obtained for all the curves between the calculated variation and the theoretical data using the same set of geometric parameters and just changing κ. It confirms that the process is controlled by the charge transfer at the graphene substrate and the process is under steady state conditions. When the potential at the substrate is rendered more and more negative, the approach curve displays a more and more positive character showing an increase of the electron transfer rate between $FcMeOH^{+}$ and the graphene layer.

Similar experiments were performed using the unsubstituted Fc and $Fc(MeOH)_2$ as redox mediators (See Figures 3 and 4) and in the two RTILs. On the whole, good agreements are also obtained between theoretical and experimental currents. As for the FcMeOH case, the positive character of the approach curves recorded increases when the potential at the substrate is rendered more negative.

Considering a Butler-Volmer model for a sufficiently negative potential versus the standard potential of the mediator, E°, k_{el} follows an exponential law with E: $\ln k_{el} = \ln k_s - \frac{\alpha F}{RT}(E - E^{\circ})$ in which k_s is the heterogeneous electron transfer standard rate constant, α is the charge transfer coefficient, F and R are the Faraday and the ideal gas constants, $(E–E^{\circ})$ is the value of the applied overpotential. The numerical values are summarized in Table 1 and plotted on Figure 5 for all mediator and RTILs.

As seen on Figure 5 that shows the plots of ln k_{el} *vs.* $(E–E^{\circ})$ for all mediators in the two ionic liquids, linear variations are obtained for large change in the driving force around 0.5 to 0.6 eV. Such linear variations may appear in agreement with Butler Volmer model, but the α values are surprisingly low and smaller than 0.1 (See Table 1) which is far from the classical value ($\alpha = 0.5$) expected for an outer-sphere electron transfer occurring for ferrocene oxidations. Additionally, the standard heterogeneous kinetics k_s are much lower than the electron transfer rate constant measured by the fast-cyclic voltammetry

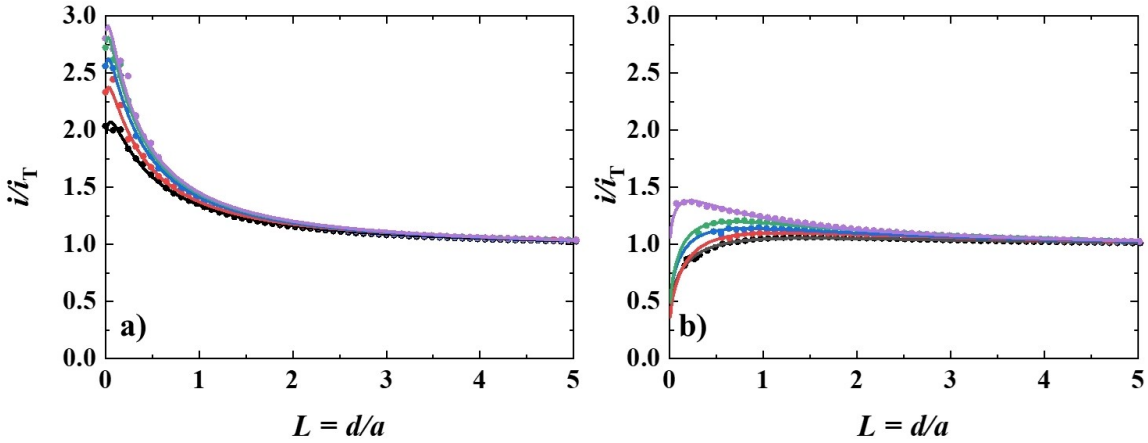

Figure 2. Experimental approach curves (points) and the corresponding fitting curve (lines) by Lefrou's formula FcMeOH in a) [EMIM][TFSI] and b) [BMIM][TFSI]. The tip potential was set on the diffusion plateau of the mediator oxidation. The substrate was biased to, from lower to upper in the figures, 0.4 (**black**, $\kappa = 2.33$), 0.3(**Red**, $\kappa = 2.24$), 0.2 V (**Blue**, $\kappa = 2.65$), 0.1 V (**Green**, $\kappa = 2.75$), and 0 V (**Purple**, $\kappa = 2.88$) in [EMIM][TFSI] and 0.4 V (**black**, $\kappa = 0.55$), 0.3 V (**Red**, $\kappa = 0.63$), 0.2 V (**Blue**, $\kappa = 0.75$), 0.0 V (**Green**, $\kappa = 0.81$), and -0.2 V (**Purple**, $\kappa = 1.30$) in [BMIM][TFSI] versus the same reference electrode. Temperature was 45 °C.

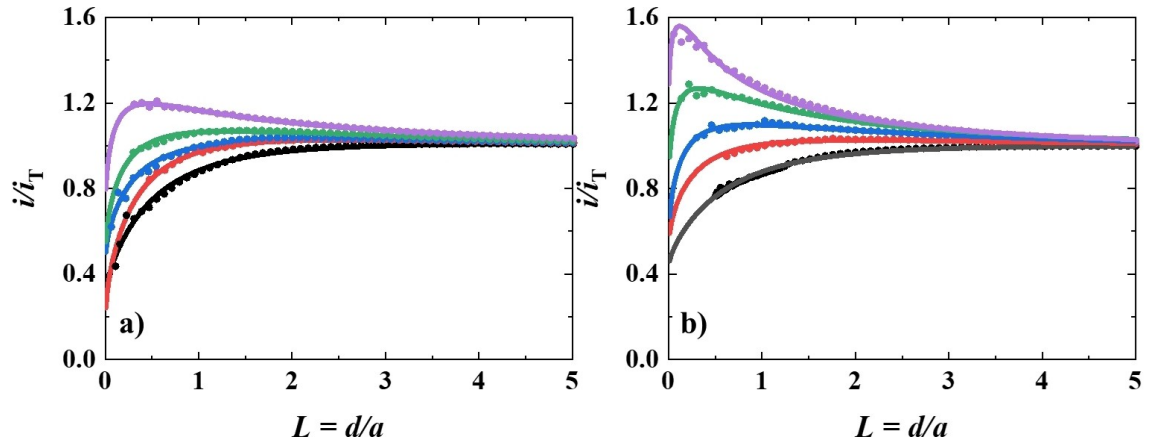

Figure 3. Experimental approach curves (points) and the corresponding fitting curve (lines) by Lefrou's formula of Fc in a) [EMIM][TFSI] and b) [BMIM][TFSI]. The tip potential was set on the diffusion plateau of the mediator oxidation. The substrate was biased to, from lower to upper in the figures, 0.2 V (**Black**, $\kappa = 0.20$), 0.1(**Red**, $\kappa = 0.36$), 0 V (**Blue**, $\kappa = 0.39$), −0.1 V (**Green**, $\kappa = 0.59$), and −0.2 V (**Purple**, $\kappa = 0.96$) in [EMIM][TFSI] and 0.4 V (**Black**, $\kappa = 0.15$), 0.3(**Red**, $\kappa = 0.44$), 0.2 V (**Blue**, $\kappa = 0.73$), 0.1 (**Green**, $\kappa = 1.12$) and 0 V (**Purple**, $\kappa = 1.65$) in [BMIM][TFSI] versus the same reference electrode. Temperature was 45 °C.

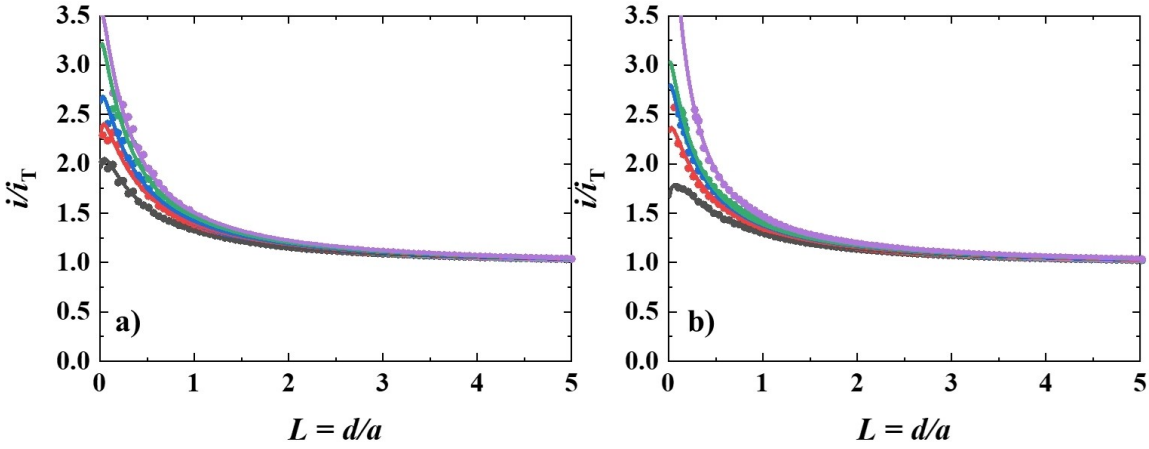

Figure 4. Probe Approaching curves (scatters) and the corresponding fitting curves (lines) by Lefrou's formula of $Fc(MeOH)_2$ in a) [EMIM][TFSI] and b) [BMIM][TFSI]. The tip potential was set on the diffusion plateau of the mediator oxidation. The substrate was biased to, from lower to upper, 0.4 V (**Black**, $\kappa = 2.38$), 0.3 V (**Red**, $\kappa = 2.52$), 0.2 V (**Blue**, $\kappa = 2.81$), 0.1 V (**Green**, $\kappa = 3.30$), and 0 V (**Purple**, $\kappa = 3.41$) in [EMIM][TFSI] and 0.4 V (**Black**, $\kappa = 1.97$), 0.3 V (**Red**, $\kappa = 2.76$), 0.2 V (**Blue**, $\kappa = 3.32$), 0.1 V (**Green**, $\kappa = 3.62$) and 0 V (**Purple**, $\kappa = 6.60$) in [BMIM][TFSI] versus the same reference electrode. Temperature was 45 °C.

for ferrocene in the same imidazolium-based ionic liquids (See below).

For identifying the specific role of the graphene from other factors that could be due to solvation of the ferrocene derivatives in the ionic liquids, we have compared the electron transfer kinetics measured on the single layer graphene with those measured using a classical 1-mm diameter disk gold electrode in the same conditions. A series of cyclic voltammograms of the ferrocene oxidations were recorded in the ionic liquids at various scan rates. Cyclic voltammetry was chosen as SECM approach curve measured with ferrocene in the same conditions but using a PPF (Pyrolyzed Photoresist Film) carbon substrate shows that the curve is controlled by the diffusion and that the rate constant is too high to be measured by SECM in our conditions. (See Figure S5 in supplementary information section). We measured the ΔE_p variations as a function of the scan rate v where ΔE_p is the difference between anodic and cathodic peak potentials. Fittings of the experimental data and calculated curves provide the parameter $\Lambda = k_s/D^{1/2}$ then the value of k_s by considering the diffusion coefficient D of the mediator assuming that the diffusion coefficient of the reduced and oxidated species are similar and a value of the transfer coefficient α close to 0.5. (See Figure 6

Table 1. Kinetic parameters of the charge transfer obtained from SECM approach curves.

Ionic Liquid	Redox probe	κ_s	α	k_s/cm s^{-1}
[EMIM][TFSI]	Fc	0.18	0.07	0.0004
	FcMeOH	2.15	0.03	0.0034
	$Fc(MeOH)_2$	1.47	0.05	0.0010
[BMIM][TFSI]	Fc	0.30	0.07	0.0001
	FcMeOH	0.38	0.05	0.0002
	$Fc(MeOH)_2$	1.77	0.05	0.0006

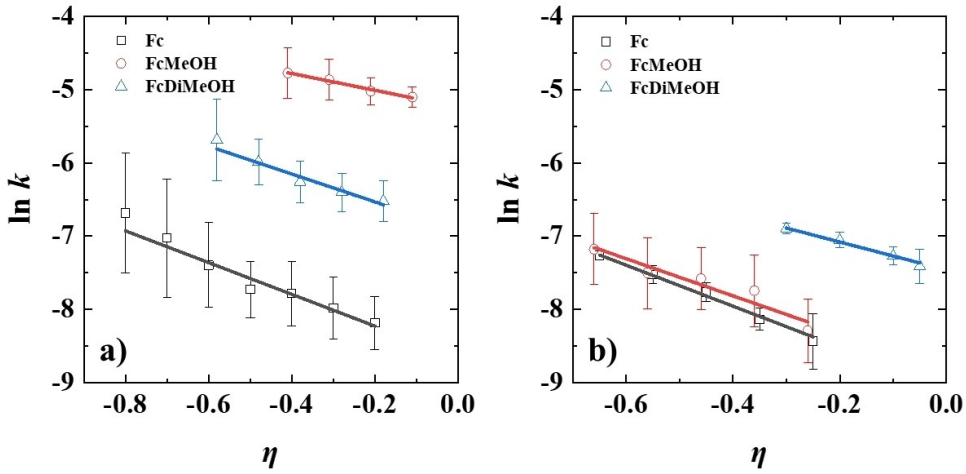

Figure 5. Plots of measured ln(k) as a function of overpotential in two ionic liquids, [EMIM][TFSI] (a) and [BMIM][TFSI](b), and three different mediators, Fc (□), FcMeOH (○) and Fc(MeOH)$_2$ (△), and the linear fitting of the corresponding data. Temperature was 45 °C.

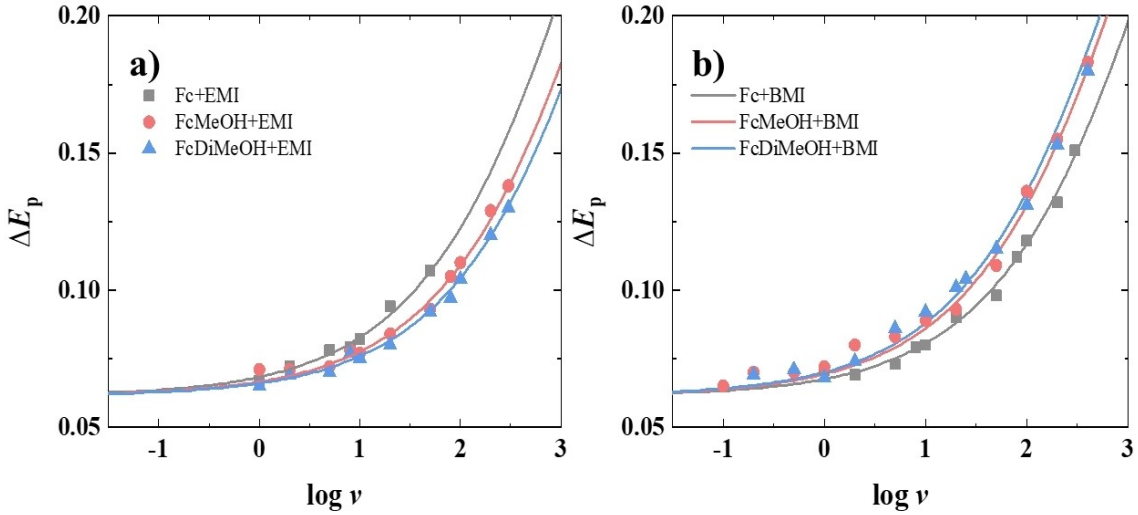

Figure 6. Fast cyclic voltammetry of the oxidation the ferrocenes using a 1-mm-diameter disk gold electrode. Variation of the peak-to-peak potential difference as function of the scan rate assuming a value the transfer coefficient $\alpha = 0.5$. Calculated curves (–) and experimental data points of the three different mediators in a) [EMIM][TFSI] and b) [BMIM][TFSI]. Temperature was 45 °C.

and Table 2) As discussed previously, the procedure requires a good compensation of the ohmic drop and the analyses of ΔE_p on sufficiently large range of scan rate. (See for example reference 23 for a discussion about the procedure). Good agreements were obtained between the expected variations and experimental data showing the quality of the procedure. The k_s rate constants are in the same range than previous reports highlighting the higher self-exchange ET rate constants for ferrocene derivatives even in ionic liquids.[14] As expected, k_s is smaller in [BMIM][TFSI] than in [EMIM][TFSI] in agreement with the more viscous character of the RTIL. However, it is remarkable that all the standard rate constants k_s measured on the single layer graphene are almost 2 orders of magnitude lower than those measured using a 1-mm diameter disk gold electrode.[14] Additionally, the cyclic voltammetry experiments show that the transfer coefficients α are not considerably different from 0.5 when using the 1-mm disk gold electrode contrarily to our results with the single layer graphene. Considering a possible artifact in the SECM analysis, we could reject the influence of the ohmic drop that

Table 2. Cyclic voltammetry. Kinetics parameters from ΔE_p/log(v) curves at a disk gold electrode.

Ionic Liquid	Redox Probe	D/cm^2.s^{-1}	k_s/cm s^{-1}
[EMIM][TFSI]	Fc	9.20×10^{-7}	0.041
	FcMeOH	5.80×10^{-7}	0.043
	Fc(MeOH)$_2$	2.51×10^{-7}	0.032
[BMIM][TFSI]	Fc	1.47×10^{-7}	0.018
	FcMeOH	1.98×10^{-7}	0.016
	Fc(MeOH)$_2$	1.20×10^{-7}	0.012

could not considerably interfere with kinetic measurements due to the small involved currents. This assumption is supported by the good agreements of the SECM curves with the calculated curves using a same set of parameters for all calculations.

We could compare the low k_s values with the data previously reported by Abruna *et al.* for different redox couples including the oxidations of FcMeOH in water and organic solvents on single layer graphene.[9] They found an apparent k_s values in the 10^{-2} cm s^{-1} range in acetonitrile ($+0.1$ mol L^{-1} NBu_4PF_6) that is a low value for a ferrocene derivative and ascribed the limited kinetics to inherent properties of graphene.[23]

Additionally, they observed very small values of the transfer coefficient α, smaller than 0.1 as in our present study in RTILs. More recently, the kinetics of the reduction of $K_3Fe(CN)_6$/$K_4Fe(CN)_6$ in water was reexamined using a single-layer graphene. It was reported that the experimental data cannot be fitted using a simple Butler-Volmer model nor with extant Marcus – Hush theory.[10] Authors express the charge transfer rate constant as a function of the density of state (DOS), which indicates specific variations with the potential in the case of single-layer graphene.[31] The discrepancies from the classical models were then attributed to be the result of dimensionality-related effects and 2D local charge density of the single-layer graphene that at the end limits the kinetics.[10] On the other hand, the limited kinetics for the charge transfer and its sensitivity to the DOS variations appear to be in the contradiction with the idea that at the energy region of the redox potential of the ferrocene derivatives, graphene possess a significant DOS.[11,12,16] Notably, the known decrease in DOS from graphite to graphene is in principle significant mainly around the intrinsic Fermi level and expected to be lower for couples with E° at a more positive potential.[32] Nevertheless, if actual model would require extended theoretical calculations to correctly describe charge transfer at single-layer graphene, our results confirm and extend the previous observations,[9,10] charge transfer kinetics on a single-layer graphene remains controlled by the intrinsic properties of the graphene layer itself even for redox couples like ferrocene derivatives. The low values of k_s and α are specific to the graphene layer and are not observed using a classical electrode in the RTILs.[33]

Conclusions

Our work illustrates the special effects on the charge transfer kinetics between a molecule and a 2D-material like a single-layer graphene. The charge transfer at a single-layer graphene/ionic liquid interface was examined using SECM. The oxidation of substituted ferrocene was chosen as model reaction due to the outer-sphere character, fast kinetics of the process and the values of their redox potentials that are far from the intrinsic Fermi level of graphene. Unexpectedly, the kinetics is characterized by slow standard charge transfer rates and an unusual low variation of the rate with the applied potential corresponding to charge transfer coefficient lower than 0.1. The observation is specific to the electrochemistry on single-layer graphene as we found that the oxidation of the same ferrocene derivatives in the same ionic liquids display a classical behavior at disk electrode in good agreement with the Butler-Volmer law. Comparison with data from literature shows that using a single layer graphene leads to considerable decrease of the charge transfer kinetics for these redox couples that could have consequence for the use of graphene materials in electrochemical applications.

Author Contributions

The manuscript was written through contributions of all authors. All authors have given approval to the final version of the manuscript. All authors contributed equally.

Acknowledgements

We thank the CNRS and the joint laboratory IRP "Nano-BioCatChem" between the three Universities and School (ENS-Paris/Rennes/Xiamen/Wuhan) for financial support. In China, this work was supported by the Natural Science Foundation of China (Nos. 22072123, 22372140) and the Chinese Scholarship Council (Nos. 202106310063).

We warmly thank Dr. Jean-François Bergamini (ISCR) for building the potentiostat with direct electronic ohmic drop compensation and his technical assistance on the scanning electrochemical microscopy.

Conflict of Interests

The authors declare no conflict of interest.

Data Availability Statement

The data that support the findings of this study are available in the supplementary material of this article.

[1] A. Ambrosi, C. Kiang Chua, A. Bonanni, M. Pumera, *Chem. Rev.* **2014**, *114*, 7150–7188.
[2] A. Ambrosi, C. K. Chua, N. M. Latiff, A. H. Loo, C. H. A. Wong, A. Y. S. Eng, A. Bonanni, M. Pumera, *Chem. Soc. Rev.* **2016**, *45*, 2458–2493.
[3] A. Yadav, M. Wehrhold, T. J. Neubert, R. M. Iost, K. Balasubramanian, *ACS Appl. Nano Mater.* **2020**, *3*, 11725–11735.
[4] N. B. Schorr, M. J. Counihan, R. Bhargava, J. Rodríguez-López, *Anal. Chem.* **2020**, *92*, 3666–3673.
[5] R. R. Nazmutdinov, M. D. Bronshtein, E. Santos, *J. Phys. Chem. C* **2019**, *123*, 12346–12354.
[6] J. Park, V. Kumar, X. Wang, P. S. Lee, W. Kim, *ACS Appl. Mater. Interfaces* **2017**, *9*, 33728–33734.
[7] N. B. Schorr, A. G. Jiang, J. Rodríguez-López, *Anal. Chem.* **2018**, *90*, 7848–7854.
[8] J. Park, V. Kumar, X. Wang, P. S. Lee, W. Kim, *ACS Appl. Mater. Interfaces* **2017**, *9*, 33728–33734.
[9] N. L. Ritzert, J. Rodríguez-López, C. Tan, H. D. Abruña, *Langmuir* **2013**, *29*, 1683–1694.

[10] R. Narayanan, H. Yamada, B. C. Marin, A. Zaretski, P. R. Bandaru, *J. Phys. Chem. Lett.* **2017**, *8*, 4004–4008.
[11] A. G. Guell, A. S. Cuharuc, Y.-R. Kim, G. Zhang, S. Y. Tan, N. Ebejer, P. R. Unwin, *ACS Nano* **2015**, *9*, 3558–3571.
[12] A. N. Patel, M. Guille Collignon, M. A. O'Connell, W. O. Y. Hung, K. McKelvey, J. V. Macpherson, P. R. Unwin, *J. Am. Chem. Soc.* **2012**, *134*, 20117–20130.
[13] M. C. Buzzeo, R. G. Evans, R. G. Compton, *ChemPhysChem* **2004**, *5*, 1106–1120.
[14] P. Hapiot, C. Lagrost, *Chem. Rev.* **2008**, *108*, 2238–2264.
[15] S. Aldroubi, N. Brun, I. Bou Malham, A. Mehdi, *Nanoscale* **2021**, *13*, 2750–2779.
[16] H. Gerischer, R. McIntyre, D. Scherson, W. Storck, *J. Phys. Chem.* **1987**, *91*, 1930–1935.
[17] K. K. Cline, M. T. McDermott, R. L. McCreery, *J. Phys. Chem.* **1994**, *98*, 5314–5319.
[18] J. H. Zhong, J. Zhang, X. Jin, J. Y. Liu, Q. Li, M. H. Li, W. Cai, D. Y. Wu, D. Zhan, B. Ren, *J. Am. Chem. Soc.* **2014**, *136*, 16609–16617.
[19] J. Molina, J. Fernández, F. Cases, *Synth. Met.* **2016**, *222*, 145–161.
[20] C. D. Hubbard, P. Illner, R. Van Eldik, *Chem. Soc. Rev.* **2011**, *40*, 272–290.
[21] R. Cornut, C. Lefrou, *J. Electroanal. Chem.* **2008**, *621*, 178–184.
[22] D. Nečas, P. Klapetek, *Open Phys.* **2012**, *10*, 181–188.
[23] F. Zhen, L. Percevault, L. Paquin, E. Limanton, C. Lagrost, P. Hapiot, *J. Phys. Chem. B* **2020**, *124(6)*, 1025–1032.
[24] D. Garreau, J. .-M. Savéant, *J. Electroanal. Chem.* **1972**, *35*, 309–331.
[25] J.-M. Savéant, *Elements of Molecular and Biomolecular Electrochemistry: An Electrochemical Approach to Electron Transfer Chemistry*, John Wiley & Sons, Inc., Hoboken, **2006**, pp. 6–52.
[26] P. Bonhôte, A. P. Diaz, N. Papageorgiou, K. Kalyasundaram, M. Grätzel, *Inorg. Chem.* **1996**, *35*, 1168–1178.
[27] D. A. Walsh, K. R. J. Lovelock, P. Licence, *Chem. Soc. Rev.* **2010**, *39*, 4185–4194.
[28] K. R. J. Lovelock, A. Ejigu, S. F. Loh, S. Men, P. Licence, D. A. Walsh, *Phys. Chem. Chem. Phys.* **2011**, *13*, 10155–10164.
[29] J. Ghilane, C. Lagrost, P. Hapiot, *Anal. Chem.* **2007**, *79(19)*, 7383–7391.
[30] S. Lhenry, Y. R. Leroux, P. Hapiot, *Anal. Chem.* **2013**, *85*, 1840–1845.
[31] H. Yamada, P. R. Bandaru, *AIP Adv.* **2016**, *6*, 065325.
[32] A. H. Castro Neto, F. Guinea, N. M. R. Peres, K. S. Novoselov, A. K. Geim, *Rev. Mod. Phys.* **2009**, *81*, 109–162.
[33] C. Lagrost, D. Carrié, M. Vaultier, P. Hapiot, *J. Phys. Chem. A* **2003**, *107(5)*, 745–752.

Manuscript received: November 10, 2023
Revised manuscript received: December 22, 2023
Version of record online: February 27, 2024